Monatsh Chem (2011) 142:789–795
DOI 10.1007/s00706-011-0521-7

ORIGINAL PAPER

Self-assembled cobalt(II) Schiff base complex: synthesis, structure, and magnetic properties

Cyril Rajnák · Ján Titiš · Roman Boča · Ján Moncol' · Zdeňka Padělková

Received: 8 February 2011 / Accepted: 2 May 2011 / Published online: 31 May 2011

Abstract A mononuclear complex $[CoL_2Cl_2]\cdot 3.5H_2O$ (L = 2-[(2,2-diphenylethylimino)methyl]pyridine-1-oxide) has been synthesized and characterized by X-ray structure analysis. The crystal structure confirms the formation of an interesting porous framework with channel diameters of about 8 Å through weak C–H···π and C–H···Cl interactions. The magnetic properties of this complex have also been studied, and the susceptibility and magnetization data were analyzed in terms of the spin Hamiltonian formalism. They confirm substantial zero-field splitting, $D/hc = 75\ cm^{-1}$.

Keywords Transition metal compounds · X-ray structure determination · Magnetic properties · UV/Vis spectroscopy

Electronic supplementary material The online version of this article (doi:10.1007/s00706-011-0521-7) contains supplementary material, which is available to authorized users.

C. Rajnák · J. Titiš (✉)
Department of Chemistry, University of SS. Cyril and Methodius, 917 01 Trnava, Slovakia
e-mail: jan.titis@ucm.sk

R. Boča · J. Moncol'
Institute of Inorganic Chemistry, Technology and Materials, Slovak University of Technology, 812 37 Bratislava, Slovakia

Z. Padělková
Department of General and Inorganic Chemistry, Faculty of Chemical Technology, University of Pardubice, Pardubice, Czech Republic

Introduction

Interest in new research into the coordination chemistry of Co(II) compounds is already substantial but is still increasing, due to their unique magnetic properties [1]. This uniqueness makes the Co(II) ion suitable for the preparation of new metal clusters with single-molecule magnet (SMM) behavior that show fascinating physical properties (such as slow magnetic relaxation and quantum tunneling) [2]. The requirements for SMMs are well known: (1) large-spin ground state; (2) large magnetic anisotropy. However, it is also very useful if such compounds possess interesting molecular or crystal structures. Much desired are, for example, molecules that are suitable for the self-assembled construction of well-ordered multidimensional structures [3].

Transition metal complexes show magnetic anisotropy as a consequence of the zero-field splitting (ZFS) that splits the states belonging to the same *S*-multiplet [4]. The zero-field splitting can be viewed at several levels of approximation. At the bottom level is the concept of the spin Hamiltonian. The spin Hamiltonian recognizes only the spin operators acting on the basis set of spin functions. The spin operators are preceded by magnetic parameters (D, E, g_z, g_x, g_y) that measure the extent of the spin–spin and spin–field interaction; these parameters are considered the molecular constants characteristic for the particular system. They can be retrieved by fitting the experimental data. The magnetic parameters originate in the electronic structure of the complex and are modulated by various structural factors of the coordination polyhedra.

The primary aim of this work was to discern correlations between the magnetic and structural properties of metal complexes. Unlike the traditional magnetostructural J correlations [5], we proposed a new type of magnetostructural

D correlation. The latter interrelates the tetragonal distortion of an octahedral pattern, D_{str}, with the axial zero-field splitting parameter *D* which results from the analysis of magnetic data. The *D* correlations were originally reported for a series of mononuclear nickel(II) complexes [6–8]. Attempts to relate structural and magnetic anisotropy in mononuclear Co(II) complexes appeared recently [9–11]. The Co(II) ion differs from the Ni(II) cases in that the ground electron term ($^4T_{1g}$) in the octahedral geometry is orbitally degenerate. On tetragonal compression it splits into the terms $^4A_{2g}$ (ground) and ^4E_g (excited), while on tetragonal elongation the opposite is true (^4E_g is the ground term) [9]. Several compounds with homogeneous and heterogeneous donor sets that are suitable for searching for magnetostructural correlations have been gradually prepared. In order to enrich this series of Co(II) complexes, we focused on bidentate Schiff base ligands possessing N and O donor atoms. Such ligands usually occupy four coordination sites in the equatorial plane, whereas the two axial positions are filled by other available donors.

Results and discussion

The title complex **1** has a composition which corresponds to the formula $[CoL_2Cl_2]\cdot 3.5H_2O$, where L is the Schiff base bidentate ligand based upon the pyridine-*N*-oxide unit. This ligand was prepared by a Schiff condensation between 2,2-diphenylethylamine and 1-oxypyridine-2-carbaldehyde at a ratio of 1:1 (Scheme 1; L = 2-[(2,2-diphenylethylimino)methyl]pyridine-1-oxide). The complex was prepared by combining $CoCl_2\cdot 6H_2O$ with purified ligand in a methanol/water solution. Pink crystals obtained within 3 days were collected by filtration. The composition and structure of **1** (Fig. 1) were determined by single-crystal X-ray analysis. Important crystallographic data are collected in Table 1.

Compound **1** crystallizes in a monoclinic system with the space group $P2_1/c$. The inversion center of this complex molecule is located at the Co(II) ion, which is positioned in a distorted octahedral environment consisting of nitrogen atoms of the azomethine group, two oxygen atoms of the *N*-oxide system (equatorial plain), and two chloride ligands

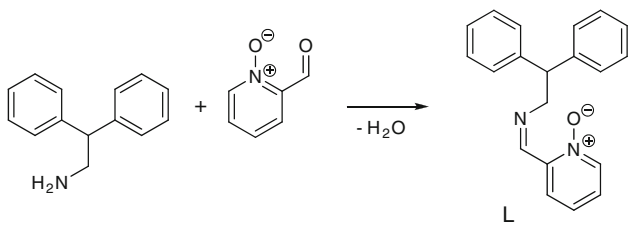

Scheme 1

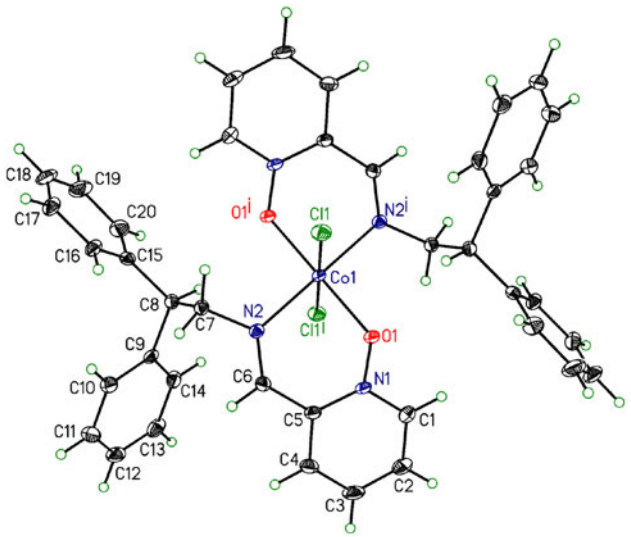

Fig. 1 ORTEP drawing of molecular complex **1** (thermal ellipsoids are drawn at the 50% probability level) [symmetry codes: (i) *x*, *y*, *z*; (ii) –*x*, *y* + 1/2, −*z* + 1/2; (iii) –*x*, −*y*, −*z*; (iv) *x*, −*y* −1/2, *z* − 1/2]

Table 1 Crystallographic data for **1**

Formula	$C_{40}H_{36}Cl_2CoN_4O_2\cdot 3.5H_2O$
Formula weight (g mol^{-1})	789.631
Crystallographic system	Monoclinic
Space group	$P2_1/c$
a (Å)	10.596(4)
b (Å)	10.535(6)
c (Å)	19.667(11)
α (°)	90.000(4)
β (°)	113.614(4)
γ (°)	90.000(4)
Volume (Å^3)	2,011.57(18)
Z	2
D_{calc} (Mg m^{-3})	1.213
μ (mm^{-1})	0.596
F(000)	762
Temperature (K)	150(2)
Reflections collected	4,059
Data/restrains/parameters	2,817/0/223
Goodness-of-fit on F^2	1.033
Final *R* indices [$I > 2\sigma(I)$]	$R = 0.0449$, $R_w = 0.0920$
Absorption correction	Empirical (*ψ*-scan)

(axial sites). The geometry of the $\{CoN_2O_2Cl_2\}$ chromophore is characterized by the bond lengths Co1–Cl1 (2.492 Å), Co1–N2 (2.081 Å), Co1–O1 (2.033 Å), and the bond angles Cl1–Co1–N2 (90.98°), O1–Co1–N2 (84.82°), Cl1–Co1–O1 (89.45°). Further important structural data are collected in Table 2. Note that the arrangements of the atoms Co, N2, C6, C5, N1, and O1 constitute a chelate ring with significant deformations. In particular, the bite angle

Table 2 Selected bond lengths and bond angles for **1**

Bond lengths (Å)			
Co1–Cl1	2.492(7)	O1–N1	1.328(3)
Co1–O1	2.033(18)	N1–C1	1.346(4)
Co1–N2	2.081(2)	N1–C5	1.365(3)
N2–C6	1.270(3)	N2–C7	1.461(3)
Bond angles (°)			
Cl1–Co1–O1	89.45(5)	N2–Co1–N2i	180.00
Cl1–Co1–N2	90.98(6)	Co1–O1–N1	119.56(14)
Cl1–Co1–Cl1i	180.00	Co1–N2–C6	124.10(17)
Cl1–Co1–O1i	90.55(5)	Co1–N2–C7	117.35(15)
Cl1–Co1–N2i	89.02(6)	N2–C7–C8	109.32(18)
O1–Co1–N2	84.82(7)	N2–C6–C5	125.20(2)
O1–Co1–O1i	180.00	C9–C8–C15	112.97(19)
O1–Co1–N2i	95.18(7)	O1–N1–C1	116.70(2)

is rather small (O1–Co1–N2 84.82°). It is evident that the effort of L to achieve an ideal bite angle (90°) subsequently deforms the O1–N1–C1 angle, the value of which is then <120° (see Table 2). Moreover, due to the flexibility of the ligand L and the electronic predispositions of sp^2 oxygen of the *N*-oxide, the pyridine units are not situated in the plane of the $\{N_2O_2\}$ donors: the dihedral angle N2–Co1–O1–N1 is ±48.23°.

For a more detailed stereochemical analysis, we utilized the parameter $D_{str} = R_{ax} - R_{eq}$ as a measure of the tetragonal distortion of the chromophore [6]. For complexes containing qualitatively different M–L bonds, the correction to the heterogeneity of the donor set reads

$$D_{str} = (d_i - \bar{d}_i)_z - [(d_i - \bar{d}_i)_x + (d_i - \bar{d}_i)_y]/2, \quad (1)$$

where $\bar{d}_i$ is the mean distance for a given bond (in this case i = N, O, Cl). Values of $\bar{d}_i$ have been taken from compounds containing $[Co(NH_3)_6]^{2+}$, $[Co(H_2O)_6]^{2+}$, and $[CoCl_6]^{4-}$ complexes, giving rise to $\bar{d}(Co-N) = 2.185$ Å, $\bar{d}(Co-O) = 2.085$ Å, and $\bar{d}(Co-Cl) = 2.475$ Å [12]. Under these assumptions, the analysis for the complex **1** yields the bond-length shifts Δ(Co–N) = −10.40 pm, Δ(Co–O) = −5.10 pm, and Δ(Co–Cl) = +1.70 pm, so the formal directions of the individual M–L vectors are $|Co–N|_{ax}$, $|Co–Cl|_{eq}$, and $|Co–O|_{eq}$, yielding $D_{str} = -8.70$ pm. This means that the effective distortion of the complex refers to a compressed tetragonal bipyramid. An analogous procedure was performed to quantify the in-plane distortion

$$E_{str} = [(d_i - \bar{d}_i)_x - (d_i - \bar{d}_i)_y]/2 \quad (2)$$

so that the rhombic structural parameter for **1** is +3.40 pm.

The most important intermolecular contacts in the crystal of **1** are presented in Fig. 2. The weak C–H···π and C–H···Cl interactions, which lead to the formation of a 3D structure, should be noted in particular. Within the unit cell, four monomeric units are connected via the C–H···π interactions to the ring (Fig. 2a). Specifically, the geometric data for these contacts are H7B···C13 2.703 Å, H6···C11 3.087 Å, H4···C19 2.851 Å, and H4···C18 2.858 Å. This interesting ring arrangement originates in the significant flexibility of the ligand L and the symmetric nature of the complex. It is then found that the packing in the *bc* plane results in a 2D network containing cavities with a diameter of about 8 Å (Fig. 2b). The complex molecules are also connected along the crystallographic *a* axis, through the C–H···Cl interactions (H3···Cl1 2.732 Å; see Fig. 2c), and ultimately form channels filled with solvent molecules (Fig. 2d).

The electronic spectrum of the studied complex shows two highly visible principal *d–d* bands in the regions 14,000–16,000 and 17,000–22,000 cm^{-1}, which are split due to the symmetry lowering of the ligand field (Fig. 3). Although the first visible *d–d* transition appears at ~10,000 cm^{-1} [$\Delta_1 = {}^4T_{2g}({}^4E_g, {}^4B_{2g}) \leftarrow {}^4T_{1g}({}^4A_{2g})$, $O_h(D_{4h})$ approximation], its intensity is weak [13]. Over 25,000 cm^{-1}, intense charge-transfer (CT) transitions are observed.

An angular overlap model (AOM) was adopted for more precise interpretation of the spectral data. To this end, a simple molecular orbital calculation based on extended Hückel theory (EHT) was performed to figure out the one-electron orbital energies for **1** using its crystallographic coordinates [14]. It has already been shown that the EHT MO energies are useful for estimating the AOM parameters e_σ and e_π [15]. In the D_{4h} symmetry approximation, the relations are: $E(z^2) = e_\sigma(xy) + 2e_\sigma(z)$, $E(x^2 - y^2) = 3e_\sigma(xy)$, $E(xz, yz) = 2e_\pi(xy) + 2e_\pi(z)$, and $E(xy) = 4e_\pi(xy)$, where E is the energy shift relative to the unperturbed *d*-orbitals. Five *d*-character EHT MOs of **1** are depicted in Fig. 4.

The energy of the *d*-orbitals in the free Co(II) ion is −13.18 eV, and thus the AOM parameters are: $e_\sigma(z) = 4{,}700$, $e_\sigma(xy) = 2{,}500$, $e_\pi(z) = 263$, and $e_\pi(xy) = 222$ cm^{-1}. The nephelauxetic ratio was set to $\beta = B/B_0 = 0.80$ (the free ion Racah parameter is $B_0 = 980$ cm^{-1}). Finally, the calculation was performed using the AOMX program [16]. The main components of the calculated energy spectrum (ideal D_{4h}) are: ${}^4A_{2g}$ (ground term), ${}^4E_g$ (644), ${}^4E_g$ (8,529), ${}^4B_{2g}$ (9,970), ${}^2E_g$ (14,021), ${}^2A_{2g}$ (14,555), ${}^4A_{2g}$ (16,543), ${}^4B_{1g}$ (16,582), and ${}^4E_g$ (19,922 cm^{-1}). Note that the distinctive bands in the 14,000–15,000 cm^{-1} region were assigned to spin-forbidden transitions to ${}^2E_g$ and ${}^2A_{2g}$ terms. We assume that these bands can borrow their intensities from the close-lying spin-allowed transitions. Above 20,000 cm^{-1}, all *d–d* transitions are spin-forbidden. According to Fig. 3, the reconstruction of the energy transitions is fairly good, so the effective tetragonal

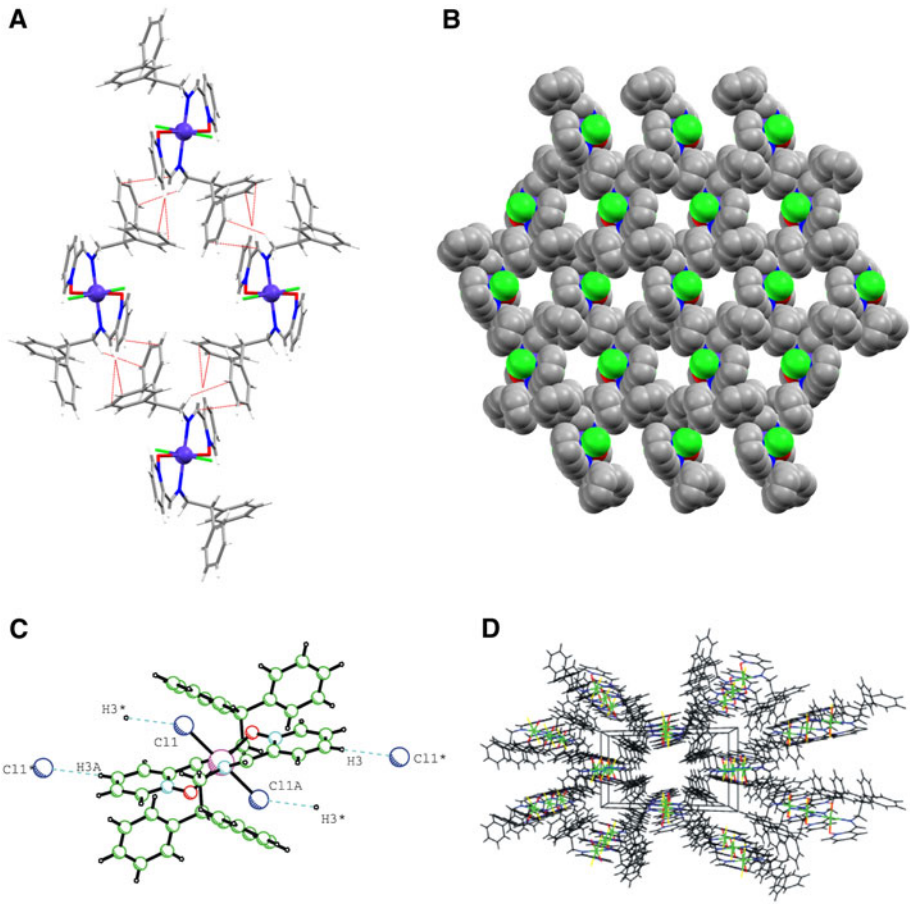

Fig. 2 Crystal packing for **1**. **a** System of C–H···π contacts in the unit cell; **b** packing in the *bc* plane; **c** C–H···Cl interactions along the crystallographic *a* axis; **d** channel formation along the crystallographic *a* axis (a perspective view)

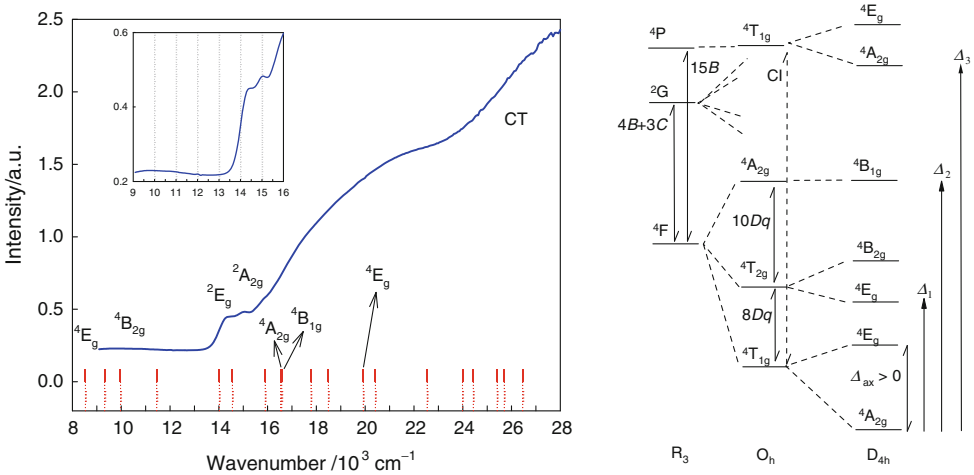

Fig. 3 Electronic *d–d* spectrum of **1** in the visible region (*left*) and the corresponding term diagram (*right*). *Vertical bars* are the calculated AOM energies of the D_{4h} terms

compression is satisfactorily confirmed. The full output of the AOMX program can be found in the Electronic supplementary material.

The magnetic data were taken with a SQUID apparatus (MPMS-XL-7, Quantum Design) in two modes: (1) temperature dependence of the magnetic susceptibility ($B_0 = 0.1$ T), which is transformed to the effective magnetic moment; (2) isothermal magnetization until $B = 7$ T, taken at $T_0 = 2.0$ and 4.6 K. The magnetic data for complex **1** are presented in Fig. 5. These show paramagnetic behavior typical of mononuclear Co(II) complexes with large zero-field splitting (ZFS). The spin-only value of the effective magnetic moment for *the* $S = 3/2$ spin system is $\mu_{\text{eff}} = 3.87\mu_B$ ($g = 2.0$). The observed value at $T = 293$ K is $\mu_{\text{eff}} = 4.35\mu_B$, showing that $g > 2$ holds true. On cooling, the effective magnetic moment stays almost constant

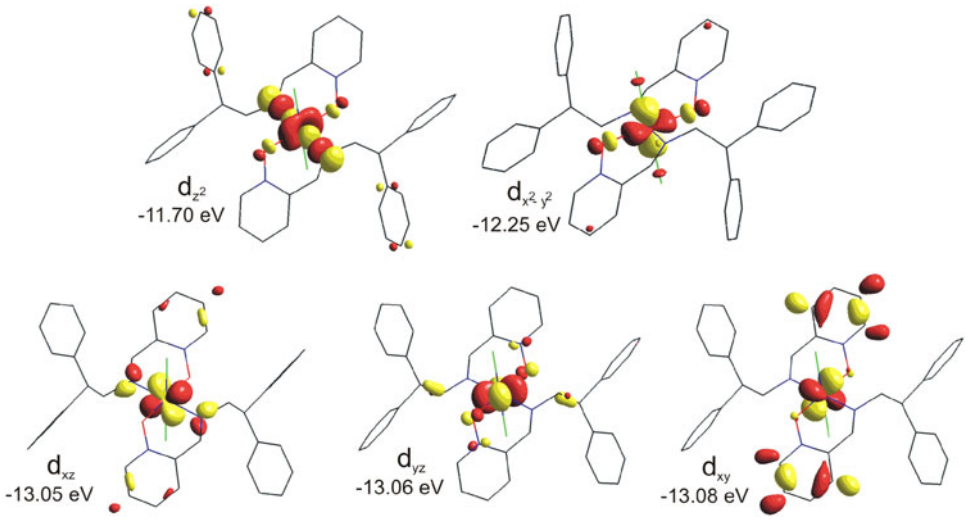

Fig. 4 *d*-Character MOs and their one-electron energies generated by the EHT method

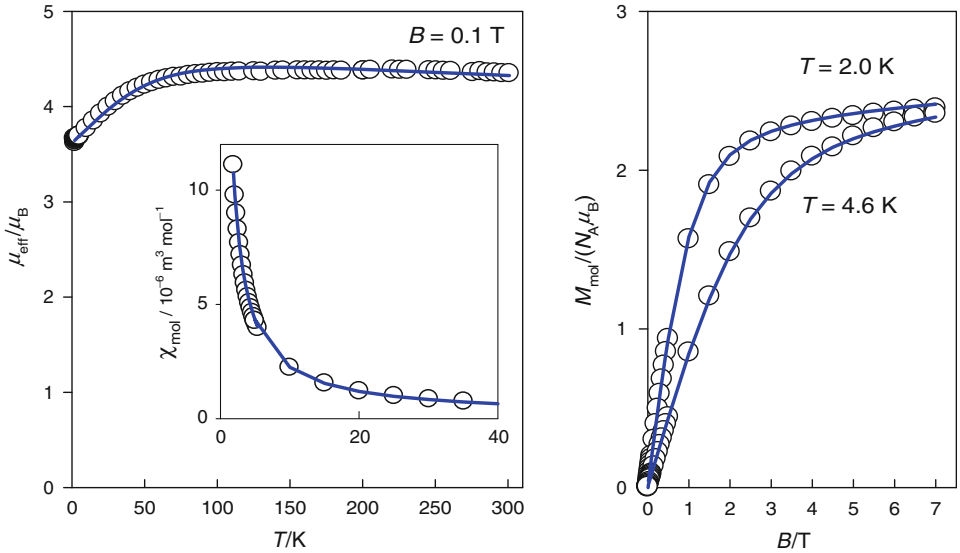

Fig. 5 Magnetic data for **1**. Temperature dependence of the effective magnetic moment (molar susceptibility) and field dependence of the molar magnetization at two temperatures. *Empty circles* experimental data, *lines* fitted

until $T = 70$ K, which reflects the Curie law. Below this temperature, the effective magnetic moment gradually decreases until a nonzero low-temperature limit. This behavior is a fingerprint of considerable zero-field splitting.

From a theoretical point of view, the magnetism of Co(II) coordination compounds is rather complex: (1) the spin-Hamiltonian formalism is fulfilled only for tetragonally compressed complexes where the $^4A_{2g}$ state refers to the ground one; (2) on approaching the octahedral limit, 12 energy levels become thermally populated (as they arise from the splitting $^4A_{2g} + {}^4E_g \leftarrow {}^4T_{1g}$), so a more complex theoretical treatment is necessary [17]. For our purpose, two independent sets of magnetic data (χ vs. T at $B = 0.1$ T and M vs. B at $T = 2.0$ and 4.6 K) were subjected to simultaneous theoretical analysis. Since the X-ray structure and the electronic spectra analysis confirmed the tetragonally compressed structure, a spin-Hamiltonian of the form

$$\hat{H}^S = \hbar^{-2}[D(\hat{S}_z^2 - \hat{S}^2/3) + E(\hat{S}_x^2 - \hat{S}_y^2)] + \hbar^{-1}\mu_B(\vec{B}\cdot\bar{\bar{g}}\cdot\vec{S}) \quad (3)$$

was used as an appropriate model. Here, D is the axial ZFS parameter, E is the rhombic ZFS parameter, and $\bar{\bar{g}}$ is the gyromagnetic ratio tensor. Other variables and symbols have their usual meanings.

In the case of high-spin d^7 systems, a theoretical analysis based upon the crystal-field approach predicts that $g_z = 2.0$ holds true [17]. A molecular-field (MF) correction improved the reproduction of the low-temperature susceptibility data. This correction was applied in the form

$$\chi_{cor} = \chi/\left[1 - \left(zj/N_A\mu_0\mu_B^2\right)\cdot\chi\right] + \alpha, \quad (4)$$

where the zj parameter accounts for the nearest neighbors. The last quantity α compensates for uncertainties in

determining the underlying diamagnetism, and it accounts for the temperature-independent paramagnetism.

An advanced fitting procedure gave the following set of magnetic parameters: $g_x = 2.356$, $g_y = 2.515$, $D/hc = 75.10\ cm^{-1}$, $E/hc = 4.84\ cm^{-1}$, $zj/hc = -0.011\ cm^{-1}$, and $\alpha = -9.01 \times 10^{-9}\ m^3\ mol^{-1}$ ($R = 0.0067$).

It is reiterated that in the solid state the magnetic anisotropy for six-coordinated Co(II) complexes adopts large values. In the case of **1**, the anisotropy values are: $D = 75.1\ cm^{-1}$ versus $D_{str} = -8.7$ pm and $E = 4.8\ cm^{-1}$ versus $E_{str} = 3.4$ pm. For instance, the results for other chromophores are: $\{CoO_6\}$, $[Co(H_2O)_6](6\text{-}OHnic)_2 \rightarrow D = 126\ cm^{-1}$ versus $D_{str} = +7.23$ pm [10]; $\{CoN_2O_2O'_2\}$, $[Co(ac)_2(H_2O)_2(MeIm)_2] \rightarrow D = 95\ cm^{-1}$ versus $D_{str} = -11.9$ pm [9]. As can be seen, the ZFS energy gap is much larger for an elongated bipyramid ($D_{str} > 0$). This is probably due to the presence of the orbital angular momentum in the effective ground term (^4E_g). According to our previous findings, these experimental relations are in good agreement with the crystal-field modeling, and could fit into the overall correlation [9].

Experimental

NMR spectra were recorded at 300 MHz for ^1H and 75 MHz for ^{13}C with a Varian Gemini 200. IR spectra were measured on a Magna FTIR 750 spectrometer (Nicolet) using KBr pellets in the 7,000–400 cm^{-1} region. Electronic spectra were measured in Nujol mull on a Specord 200 (Analytical Jena) in the range 50,000–9,000 cm^{-1}. Magnetic susceptibility and magnetization measurements were done using a SQUID magnetometer (Quantum Design) from 2 K at $B = 0.1$ T. The magnetization data were taken at $T = 2.0$ and 4.6 K. Raw susceptibility data were corrected for underlying diamagnetism using the set of Pascal constants. The effective magnetic moment was calculated in the usual manner: $\mu_{eff}/\mu_B = 798(\chi' T)^{1/2}$ when SI units are employed.

The crystallographic data collection was carried on a Bruker–Nonius Kappa CCD diffractometer equipped with graphite-monochromatized Mo Kα ($\lambda = 0.71073$ Å) using EvalCCD software [18]. The numerical absorption correction was applied using the Gaussian integration method. The structure was solved by a direct method using SIR-97 [19] and refined on F^2 by full-matrix least squares using SHELXL-97 [20]. The crystal structure contained disordered solvent molecules, amounting to 140 electrons per unit cell. Their contribution to the structural factors was evaluated by back Fourier transformation with PLATON-SQUEEZE [21]. CCDC 796703 contains the supplementary crystallographic data for **1**. These data can be obtained free of charge via http://www.ccdc.ac.uk/conts/retrieving.html, or from the Cambridge Crystallographic Data Centre (12 Union Road, Cambridge CB2 1EZ, UK; fax: (+44) 1223-336-033; or e-mail: deposit@ccdc.cam.ac.uk).

2-[(2,2-Diphenylethylimino)methyl]pyridine-1-oxide) ($C_{20}H_{18}N_2O$)

An amount of 0.66 g 1-oxypyridine-2-carbaldehyde (4.68 mmol) dissolved in 20 cm^3 methanol were added to 0.92 g of 2,2-diphenylethylamine (4.68 mmol) dissolved in 20 cm^3 methanol. The mixture was refluxed for 30 min, cooled, and filtered. Recrystallization from ethanol afforded 0.90 g (60%) as yellow crystals. M.p.: 114 °C; ^1H NMR (300 MHz, DMSO-d_6): $\delta = 4.38$ (C9, 2H, d), 4.59 (C10, 1H, t), 7.27 (CH^{Ar}, 1H, dddd), 7.39 (C5, 1H, ddd), 7.51 (C2, 1H, ddd), 7.72 (C3, 1H, ddd), 8.16 (C7, 1H, s) ppm; ^{13}C NMR (75 MHz, DMSO-d_6): $\delta = 42.9$ (C10), 62.3 (C9), 125.2 (CH^{Ar}), 135.8 (C3), 143.1 (C11, C18), 149.9 (C5), 163.7 (C7) ppm; IR (KBr): $\bar{\nu} = 754$ (Ar–H, wag), 1,291 (N–O, stretch), 1,636 (C=N, stretch) cm^{-1}.

Bis[2-[(2,2-diphenylethylimino)methyl]pyridine-1-oxide)]cobalt(II)dichloride hydrate
(**1**, $C_{40}H_{36}Cl_2CoN_4O_2{\cdot}3.5H_2O$)

An amount of 0.12 g $CoCl{\cdot}6H_2O$ (0.50 mmol) dissolved in 10 cm^3 methanol + water were added to 0.30 g 2-[(2,2-diphenylethylimino)methyl]pyridine-1-oxide) (1.0 mmol) dissolved in 30 cm^3 methanol. The mixture was refluxed for 2 h, cooled, and filtered. Dark pink block-shaped crystals were grown by evaporating the solution within 3 days. The yield was 0.17 g (57%).

Acknowledgments Slovak Grant Agencies (VEGA 1/1005/09, 1/0052/11 and APVV-VVCE-0004-07) and the Ministry of Education of the Czech Republic (Project VZ0021627501) are acknowledged for their financial support of this work.

References

1. Lloret F, Julve M, Cano J, Ruiz-García R, Pardo E (2008) Inorg Chim Acta 361:3432
2. Murrie M (2010) Chem Soc Rev 39:1986
3. Atwood JL, Barbour LJ, Jerga A (2002) Science 296:2367
4. Kahn O (1993) Molecular magnetism. VCH, New York
5. Gorun SM, Lippard SJ (1991) Inorg Chem 30:1625
6. Mašlejová A, Ivaniková R, Svoboda I, Papánková B, Dlháň L', Mikloš D, Fuess H, Boča R (2006) Polyhedron 25:1823
7. Boča R, Titiš J (2008) Magnetostructural *D*-correlations for zero-field splitting in nickel(II) complexes. In: Cartere TW, Verley KS (eds) Coordination chemistry research progress. Nova, New York, p 247
8. Titiš J, Boča R (2010) Inorg Chem 49:3971
9. Papánková B, Boča R, Dlháň L', Nemec I, Titiš J, Svoboda I, Fuess H (2010) Inorg Chim Acta 363:147
10. Segl'a P, Miklovič J, Mikloš D, Titiš J, Herchel R, Moncol' J, Kaliňáková B, Hudecová D, Mrázová V, Lis T, Melník M (2008) Transition Met Chem 33:967
11. Segl'a P, Miklovič J, Mikloš D, Mrázová V, Krupková V, Hudecová D, Ondrušová Z, Švorec J, Moncol' J, Melník M (2009) Transition Met Chem 34:15

12. FIZ Karlsruhe (2011) Inorganic Crystal Structure Database. Fachinformationszentrum Karlsruhe, Karlsruhe. http://www.fiz-informationsdienste.de/en/DB/icsd/index.html
13. Lever ABP (1984) Inorganic electronic spectroscopy, 2nd edn. Elsevier, Amsterdam
14. Hypercube, Inc. (2011) HyperChem. Hypercube, Inc., Gainesville
15. Baba H, Nakano M (2009) Polyhedron 28:2087
16. Adamsky H (1982) AOMX—a Fortran computer program for ligand field calculations within the angular overlap model. Heinrich-Heine Universität, Düsseldorf
17. Boča R (2006) Struct Bonding 117:1
18. Duisenberg AJM, Kroon-Batenburg LMJ, Schreurs AMM (2003) J Appl Cryst 36:220
19. Altomare A, Burla MC, Camalli M, Cascarano GL, Giacovazzo C, Guagliardi A, Moliterni AGG, Polidori G, Spagna R (1999) J Appl Cryst 32:115
20. Sheldrick GM (2008) Acta Cryst A64:112
21. van der Sluis P, Spek AL (1990) Acta Cryst A46:194